

# A Combinatorial Library of Bi-functional Polymeric Vectors for siRNA Delivery *In Vitro*

Jeisa M. Pelet • David Putnam

Received: 14 April 2012 / Accepted: 23 August 2012 / Published online: 28 September 2012  
© Springer Science+Business Media, LLC 2012

## ABSTRACT

**Purpose** To apply a combinatorial chemistry approach toward the design of polymeric vectors, and to evaluate their effectiveness as siRNA delivery systems *in vitro*.

**Methods** Poly(acrylic acid) (pAA) was synthesized via RAFT polymerization with well-controlled molecular weights ( $M_n$ : 3 kDa, 5 kDa, 10 kDa and 21 kDa). A polymer library was generated from the pAA precursors by conjugating two distinct moieties, agmatine (Agm) and D-(+)-galactosamine (Gal), at various ratios. Biophysical and cellular characterization was evaluated *in vitro* for these polymeric vectors using MDA-MB-231-luc+ cells.

**Results** A critical balance between Agm/Gal content and polymer molecular weight must be attained to achieve favorable transfection efficacies. From the library of 22 polymers, only a few had knockdown efficiencies commensurate with effective siRNA delivery, particularly those with polymer precursor  $M_n$  of 5 kDa and 10 kDa. Highest protein knockdown of 84% was achieved by a polymer conjugate with a 5 kDa pAA backbone with a side chain composition of 55% Agm and 17% Gal.

**Conclusions** Effective delivery of siRNA was found to be highly dependent on the molecular structure of the polymeric vector. The combinatorial approach employed provided the tools to identify optimal structural properties leading to efficient siRNA delivery for this class of vector.

**KEY WORDS** combinatorial libraries • luciferase • polymeric vectors • siRNA delivery

## ABBREVIATIONS

Agm	agmatine
FA	fluoresceinamine
Gal	D-(+)-galactosamine
$M_n$	number-average molecular weight
pAA	poly(acrylic acid)
PDI	polydispersity index
PEIb	branched polyethyleneimine
siRNA	small interfering RNA

## INTRODUCTION

The discovery of RNA interference (1) (RNAi) has led to a revolution in molecular biology and disease treatment. RNAi is a highly regulated post-transcriptional mechanism that modulates protein expression, and has become attractive for studies involving protein regulation both *in vitro* and *in vivo* (2–4). By taking advantage of this endogenous mechanism, gene silencing can be induced by sequence-specific cleavage of a messenger RNA, thereby reducing or eliminating undesired protein expression. Inducing protein knockdown in mammalian systems can be achieved using different effectors, including synthetic small interfering RNA (siRNA), short hairpin RNA (shRNA), and DNA encoding for shRNA (5). In particular, synthetic siRNA, generally composed of oligonucleotides 21–23 base pairs long, offers significant advantages over other effectors such as a wide range of mRNA targets with high specificity and a cytoplasmic site of action, thereby avoiding chromosomal DNA perturbations.

Introducing siRNA into cells is challenging owing to the lack of effective delivery vectors that can safely transport

**Electronic supplementary material** The online version of this article (doi:10.1007/s11095-012-0876-4) contains supplementary material, which is available to authorized users.

J. M. Pelet • D. Putnam  
School of Chemical and Biomolecular Engineering, Cornell University  
Ithaca, New York 14853, USA

D. Putnam (✉)  
Department of Biomedical Engineering, Cornell University  
147 Weill Hall  
Ithaca, New York 14853, USA  
e-mail: dap43@cornell.edu

these macromolecules to their site of action while overcoming a manifold of the barriers that hinder the delivery pathway (6). In contrast to viral vectors, non-viral delivery systems have become promising therapeutic alternatives due to their low cytotoxicity profiles, low immunogenic potential and ease of chemical modifications. Among non-viral delivery systems, polymer-based vectors have gained increasing attention primarily due to the ability to tailor their architectures, and consequently their physicochemical properties, for specific applications (7–9). Although several drawbacks exist for polymeric vectors, they can be designed to integrate specific functionalities that provide beneficial properties including cell targeting, pH-responsiveness, and thermodynamic stability in the extracellular medium. Multifunctional polymers are adaptable to address multiple design criteria for bioactive materials (10); however, identifying optimal structural characteristics from a wide structure-parameter space can be challenging.

Combinatorial libraries of polymers have become a valuable avenue for the design of functional biomaterials, particularly for gene delivery (11–17). Through combinatorial libraries, the structure-function relationship of biomaterials can be correlated to identify the most favorable structural parameters for optimal outcomes—in this case, high transfection efficiencies with minimal cytotoxicity. Therefore, a combinatorial approach can be remarkably powerful for the development of bioactive polymers as siRNA delivery systems. Moreover, branched polymers, such as poly(acrylic acid) (pAA), offer the flexibility for structural modifications due to their multiple side chains. Following a similar chemistry, various moieties could potentially be incorporated, therefore enhancing the ability to generate new functional biomaterials.

In this study, a combinatorial chemistry approach was applied toward the design of polymeric vectors for enhanced siRNA delivery through an analysis of their structure-function relationships. Toward this goal, pAA of different molecular weights ( $M_n$ ) was synthesized by reversible addition-fragmentation chain transfer (RAFT) polymerization. Based on these pAA precursors, a library of polymers was generated by the side chain substitutions with two distinct moieties, agmatine (Agm) and D-(+)-galactosamine (Gal), at varying ratios. Agm provides a cationic source to facilitate interactions with the siRNA and enhance cell membrane permeability, while Gal can serve as a polyplex solubilizer/stabilizer. The structural parameters examined include: 1) molecular weight ( $M_n$ ) of the polymer; 2) Agm content; and 3) Gal content. The biophysical and cellular characterization of these polymeric vectors was carried out and herein reported, including the relative binding affinity of the polymers with siRNA, polyplex stability in the presence of competitive ionic species (sodium heparin), polyplex stability in serum, polyplex effective diameter and zeta

potential, cytotoxicity and transfection efficiency using MDA-MB-231-luc+ cells as a model cell line.

## MATERIALS AND METHODS

### Materials

25 kDa branched polyethylenimine (PEIb), sodium heparin from porcine intestinal mucosa, fluoresceinamine, isomer I (FA), bovine serum albumin (BSA) and ethidium bromide (EtBr) were purchased from Sigma-Aldrich. HEPES buffer (10 mM, pH 7.2) was prepared with ultrapure water and filtered through a 0.2  $\mu$ m PES membrane. TBE buffer (0.089 M Tris base, 0.089 M boric acid, and 2 mM sodium EDTA) and SYBR green II RNA gel stain were purchased from Invitrogen. MDA-MB-231-luc+ cells (human breast carcinoma cell line), kindly donated by Dr. Balraj Singh, University of Texas MD Anderson Cancer Center, Houston Texas, were maintained in Dulbecco's Modified Eagle Medium (DMEM Cellgro, Mediatech Inc., Manassas VA) with 10% *v/v* Fetal Bovine Serum (FBS, HyClone, Thermo Scientific) and no antibiotics at 37°C and 5% CO<sub>2</sub>. Luciferase GL3 duplex siRNA (sense sequence 5'-CUU ACG CUG AGU ACU UCG A dTdT -3') and non-specific control duplex siRNA (sense sequence 5'-AUG UAU UGG CCU GUA UUA G UU -3'), were purchased from Dharmacon, Thermo Scientific. Costar 96-well plates (clear and opaque) were purchased from Corning Life Sciences.

### Characterization

$M_n$  and polydispersity indices (PDI) for pAA were obtained using a Waters Gel Permeation Chromatography (GPC) system equipped with two Ultrahydrogel™ columns (Waters) in series (500 Å and 250 Å), 1515 isocratic HPLC pump and 2414 refractive index detector with the temperature controlled at 30°C. The mobile phase employed was phosphate buffer saline (pH=7.4) at a rate of 0.8 mlmin<sup>-1</sup> calibrated with poly(methacrylic acid), sodium salt standards. <sup>1</sup>H NMR of pAA and polymer conjugates was performed using an Inova 400 MHz spectrometer with deuterium oxide (D<sub>2</sub>O) as the solvent. Resonances were referenced to HOD at 4.81 ppm. Particle effective diameter and zeta potential were obtained with a Malvern Zetasizer Nano-ZS system using the Malvern Dispersion Technology software supplied by the instrument manufacturer. The Smoluchowski model was applied to calculate zeta potentials. Confocal imaging was performed on a Leica TCS SP2 laser scanning confocal system with a HCX PL APO 63x/1.32–0.6 oil immersion CS objective equipped with a 4-line argon laser. Gel electrophoresis was performed in an Invitrogen XCell SureLock™ Mini-Cell using Novex® 15%

TBE-urea pre-cast gels. Gels were run at a constant voltage of 200 V. Absorbance was obtained using a Molecular Devices SpectraMax Plus<sup>384</sup> UV/Vis spectrophotometer at the specified wavelength ( $\lambda_{\text{abs}}$ ). Fluorescence was obtained using a Molecular Devices SpectraMax GeminiEM at the specified excitation and emission wavelengths ( $\lambda_{\text{exc}}$  and  $\lambda_{\text{emi}}$ , respectively). Luminescence (in RLU units) was obtained using a Veritas Microplate Luminometer (Turner Biosystems).

### Polymer Precursor Synthesis

pAA of various  $M_n$  were synthesized as previously reported by our group (18). A representative example for 3 kDa pAA (Table I, entry 1–6) is as follows: Acrylic acid (AA; 0.950 ml, 13.9 mmol) and 4-cyanopentanoic acid dithiobenzoate (CPA-DB; 77.8 mg, 0.278 mmol; in 3.0 ml methanol) were transferred to a 5 ml glass ampule with a magnetic stirbar and purged with nitrogen for 5 min. 4,4'-azobis(4-cyanopentanoic acid) (A-CPA; 19.5 mg, 0.0695 mmol; in 0.670 ml methanol) was added, and the solution was purged with nitrogen for 2 min. The ampule was flame-sealed and polymerization initiated with continuous stirring (600 rpm) at 60°C. The reaction was stopped at 48 h by inserting the ampule in an ice bath and exposing the solution to air. The solution was then placed under reduced pressure (Edwards RV8 vacuum pump) for 15–20 min, diluted with deionized-water and dialyzed using Spectra/Por regenerated cellulose dialysis tubing (1 kDa MWCO) against deionized-water for 3 days. The product was recovered by lyophilization. For this particular sample,  $M_n=2,900$ , PDI=1.36 and percent conversion estimated by gravimetric analysis was 37%. <sup>1</sup>H NMR (D<sub>2</sub>O, ppm) pAA:  $\delta$  1.8 (br t, 2H),  $\delta$  2.4 (br s, 1H).

### Polymer Conjugate Synthesis

Polymer conjugates were synthesized by a sequential conjugation of Agm and Gal to the side chains of pAA as previously reported by our group (18). The conjugation of these groups was mediated via a condensation reaction using 4-(4,6-dimethoxy-1,3,5-triazin-2-yl)-4-methylmorpholinium chloride (DMTMM) as the condensing agent. Briefly, a representative example for 200% (mol percentage) target Agm conjugation to 3 kDa pAA (3-P1), which corresponds to  $[\text{COOH}]_0:[\text{DMTMM}]_0:[\text{Agm}]_0=1:2:4$  (Table I, entry 1) is as follows: pAA (50 mg, 0.69 mmol COOH) and Agm (640 mg, 2.8 mmol) were transferred to a 25 ml pear-shaped flask with a magnetic stir bar, dissolved with 13 ml of 0.1 M borate buffer, pH=8.5 and stirred for 10 min. A DMTMM solution (390 mg, 1.4 mmol; in 3.7 mL of 0.1 M borate buffer, pH=8.5) was added dropwise, and the pH was adjusted to 8.0 with additions of 1 N sodium hydroxide (NaOH). The reaction flask was capped and continuously

stirred (600 rpm) at room temperature for 48 h. The product was purified by dialysis using Spectra/Por regenerated cellulose dialysis tubing (1 kDa MWCO) against 0.001 M borate buffer (pH=8.5) for 2 days and deionized-water for 2 additional days and recovered by lyophilization. For this particular sample, Agm actual substitution to pAA was 76% which corresponds to a conjugation efficiency of 38%. <sup>1</sup>H NMR (D<sub>2</sub>O, ppm) pAA-Agm:  $\delta$  1.6 (s, 4H),  $\delta$  1.7 (br s, 2H),  $\delta$  2.1 (br s, 1H),  $\delta$  3.2 (s, 4H). Sequential conjugation of Gal to pAA-Agm followed the same procedure as previously described with  $[\text{polymer}]_0=3.0$  mg/ml and the pH adjusted to 7.0 with additions of 1N sodium chloride (HCl). The product was purified by dialysis using Spectra/Por regenerated cellulose dialysis tubing (1 kDa or 3.5 kDa MWCO) against water for 3 days and recovered by lyophilization. <sup>1</sup>H NMR (D<sub>2</sub>O, ppm) pAA-Agm-Gal:  $\delta$  1.6 (s, 4H),  $\delta$  1.7 (br s, 2H),  $\delta$  2.1 (br s, 1H),  $\delta$  3.2 (s, 4H),  $\delta$  3.5–4.7 (m, 6H). To obtain different ligand contents, the  $[\text{COOH}]_0$  to  $[\text{DMTMM}]_0$  molar ratio was varied with  $[\text{NH}_2]_0=2 \cdot [\text{DMTMM}]_0$  and  $[\text{polymer}]_0=3.0$  mg/ml (Supplementary Table S1, Table S2 and Table S3). The degree of side chain substitution of each ligand (mol %) in pAA was determined by <sup>1</sup>H NMR (400 MHz, D<sub>2</sub>O) through integration of the <sup>1</sup>H NMR resonances (Supplementary Material).

### Fluoresceinamine Conjugation to Polymer Conjugates

A representative example for 10% (mol percentage) target FA conjugation to available carboxyl groups in 10 kDa pAA-78%Agm-3%Gal (10-P2), which corresponds to  $[\text{COOH}]_0:[\text{DMTMM}]_0:[\text{FA}]_0=1:0.1:0.2$  is as follows: 10-P2 (10 mg, 0.012 mmol COOH) and FA (0.83 mg, 0.0024 mmol in 33  $\mu$ l of DMSO) were transferred to a 5 ml pear-shaped flask with a magnetic stir bar, dissolved with 2 ml of 0.1 M borate buffer, pH=8.5 and stirred for 10 min. A DMTMM solution (0.33 mg, 0.0012 mmol; in 1.3 ml of 0.1 M borate buffer, pH=8.5) was added dropwise, and the pH was adjusted to 7.5 with additions of 1N NaOH. The reaction flask was capped and continuously stirred (600 rpm) at room temperature for 24 h. The product was purified by dialysis using Spectra/Por regenerated cellulose dialysis tubing (3.5 kDa MWCO) against deionized-water for 3 days and recovered by lyophilization.

### Preparation of Polyplexes

A 0.5 mg/ml stock solution of each polymer conjugate was prepared with 10 mM HEPES buffer, pH 7.2. Immediately prior to formation of the polyplex, the polymer conjugate stock solution was sonicated for 60 sec to disrupt electrostatic interaction between polymer chains prior to complexation with the siRNA. A specific volume of a 20  $\mu$ M or 2  $\mu$ M siRNA stock solution was mixed with aliquots of the

**Table 1** Polymer Precursor (pAA)  $M_n$  and PDI, Agm Content and Gal Content for Polymer Conjugates

Entry	Name		pAA $M_n^a$	PDI <sup>a</sup>	Agm Content (%) <sup>b</sup>	Gal Content (%) <sup>b</sup>
1	3 kDa-P	3-P1	2 900	1.36	76	0
2		3-P2			76	3
3		3-P3			56	17
4		3-P4			56	8
5		3-P5			45	22
6		3-P6			45	13
7	5 kDa-P	5-P1	4 800	1.32	76	0
8		5-P2			76	2
9		5-P3			55	17
10		5-P4			55	10
11		5-P5			46	28
12		5-P6			46	14
13	10 kDa-P	10-P1	10 400	1.20	78	0
14		10-P2			78	3
15		10-P3			56	18
16		10-P4			56	10
17		10-P5			46	26
18		10-P6			46	14
19	21 kDa-P	21-P1	20 900	1.19	72	0
20		21-P2			72	3
21		21-P3			55	12
22		21-P4			55	4

<sup>a</sup>As determined by Gel Permeation Chromatography (GPC)

<sup>b</sup>As determined by <sup>1</sup>H NMR (400 MHz, D<sub>2</sub>O)

polymer conjugates stock solution to form the designated polymer:siRNA (w:w) ratio. The final volume was adjusted to 120  $\mu$ L, unless otherwise specified, with 10 mM HEPES buffer, pH 7.2. After vortexing for 5 sec, the polyplex solution was incubated at room temperature for 20 min.

### Relative Polyplex Binding Affinity and Competitive Displacement with Heparin

The relative strength of electrostatic binding between siRNA and polymer conjugates and the displacement of siRNA from the polyplex by heparin (competitive anionic species) were measured by EtBr fluorescence quenching. Stock solutions of siRNA, polymer conjugates, sodium heparin, and EtBr were prepared with 10 mM HEPES buffer, pH 7.2. Polyplexes were formed as previously described. siRNA (20  $\mu$ l of a 2  $\mu$ M stock solution) was combined with a specific volume of the polymer conjugate stock solution to achieve the designated polymer:siRNA (w:w) ratio, and the final volume was adjusted to 120  $\mu$ l with 10 mM HEPES buffer, pH 7.2. The polyplex solution (100  $\mu$ l) was transferred to a black 96-well polystyrene plate (non-treated).

For the relative binding affinity assay, EtBr (50  $\mu$ l of a 14  $\mu$ M stock solution) was added to each well, and the plates were incubated at room temperature for 20 min. For the competitive heparin displacement assay, a sodium heparin

solution (10  $\mu$ l) of varying concentrations was transferred to each corresponding well, and plates were incubated at 37°C for 20 min. EtBr (40  $\mu$ l of a 17.5  $\mu$ M stock solution) was added to each well, and plates were incubated at room temperature for an additional 20 min.

The final concentration of EtBr was 4.67  $\mu$ M and the siRNA phosphate group to EtBr molar ratio was 2:1. Fluorescence was read at  $\lambda_{exc}$ =535 nm and  $\lambda_{emi}$ =595 nm. Each condition was performed in triplicate.

### Polyplex Stability in Serum

The polyplex stability in the presence of serum proteins was evaluated as previously described by Katas *et al.* (19). Briefly, polyplexes were formed as previously described. siRNA (18.8  $\mu$ l of a 20  $\mu$ M stock solution) was combined with a specific volume of the polymer conjugate stock solution to achieve the designated polymer:siRNA (w:w) ratio, and the final volume was adjusted to 200  $\mu$ l with 10 mM HEPES buffer, pH 7.2. Polyplexes were incubated at 37°C with an equal volume of DMEM with 20% v/v FBS. The FBS final concentration was 10% v/v. At the designated times (0, 1, 2, 4, 8, 16, 24 and 48 h), an aliquot of the polyplex solution (40  $\mu$ l) was removed, flash frozen in liquid nitrogen and stored at -80°C. To terminate serum activity and to dissociate the siRNA from the complex, samples were incubated

at 80°C for 5 min and sodium heparin (5  $\mu$ l of a 1 mg/ml stock solution) was added, respectively. The integrity of the siRNA was assessed by gel electrophoresis using a 15% TBE-urea polyacrylamide gel (Invitrogen) at a constant voltage of 200 V for 1 h in 1x TBE buffer. Gels were afterward incubated in SYBR green II RNA gel stain (1:10,000 dilution in ultrapure water filtered through a 0.2  $\mu$ m PES membrane) for 40 min, and siRNA bands were visualized under a UV transilluminator ( $\lambda$ =302 nm) using a SYBR Green gel stain photographic filter (Invitrogen).

### Effective Diameter and Zeta Potential

Polyplexes were formed as previously described. siRNA (19.8  $\mu$ l of a 20  $\mu$ M stock solution) was combined with a specific volume of the polymer conjugate stock solution to achieve the designated polymer:siRNA (w:w) ratio, and the final volume was adjusted to 1.05 ml with 10 mM HEPES buffer, pH 7.2 (50  $\mu$ l and 1 ml for effective diameter and zeta potential measurements, respectively). The siRNA final concentration was 5  $\mu$ g/ml. Effective diameter and zeta potential of polyplexes were determined by dynamic light scattering using a Malvern Zetasizer Nano-ZS. For the particle effective diameter, three measurements consisting of 10 runs of 10 s each were performed on each sample at room temperature. For the particle zeta potential, three measurements consisting of 15 runs each were performed on each sample at room temperature.

### Confocal Microscopy

MDA-MB-231-luc+ cells ( $1 \times 10^6$  cells/plate) were seeded in 2 ml of growth medium (DMEM with 10% *v/v* FBS) in polystyrene plates (non-treated, 60 mm $\times$ 15 mm) with 3 glass coverslips (non-treated, 12 mm diameter) 24 h prior to transfection and incubated at 37°C and 5% CO<sub>2</sub>. Immediately prior to transfection, polyplexes were formed as previously described. siRNA (11.3  $\mu$ l of a 20  $\mu$ M stock solution) was combined with a specific volume of the FA-labeled polymer conjugates stock solution (10-P2-FA or 10-P3-FA) to achieve the designated polymer:siRNA (w:w) ratio, and the final volume was adjusted to 310  $\mu$ l with 10 mM HEPES buffer, pH 7.2. After formation of the polyplex, 4.19 ml of serum-free medium was added to the polyplex solution. The growth medium was removed from the plates, and cells were rinsed with 1 $\times$  Dulbecco's phosphate buffered saline (DPBS, Cellgro, Mediatech Inc., Manassas VA, 2 ml). The glass coverslips were transferred to new plates with 2 ml of serum-free medium (3 coverslips/plate), corresponding to 120,000 cells/plate. The serum-free medium from the plates was replaced with 2.25 ml of the polyplex solution. The siRNA concentration per plate was 0.67  $\mu$ g/ml (1.5  $\mu$ g siRNA per plate). Plates were incubated

at 37°C and 5% CO<sub>2</sub> for 4 h. Cells were rinsed 3 times with DPBS (2 ml), fixed with 3.7% formaldehyde (2 ml) for 10 min followed by quenching with BSA (2 ml of 10 mg/ml in DPBS). Coverslips were mounted onto microscopy slides using Vectashield mounting medium (Vector Laboratories, Burlingame CA), and cells were immediately imaged using a Leica TCS SP2 laser scanning confocal system. FA-containing polymer conjugates were detected by excitation at 488 nm, and fluorescence emission was collected at 500–550 nm.

### Cytotoxicity

MDA-MB-231-luc+ (8,000 cells/well) were seeded in 100  $\mu$ l of growth medium (DMEM with 10% *v/v* FBS) in clear 96-well polystyrene plates (tissue-culture treated) 24 h prior to transfection and incubated at 37°C and 5% CO<sub>2</sub>. A 0.5 mg/ml polymer stock solution was prepared with 10 mM HEPES buffer, pH 7.2 and sonicated for 60 sec to disrupt electrostatic interactions between polymer chains. From this stock solution, polymer conjugates were diluted with 10 mM HEPES buffer, pH 7.2 to various concentrations at a final volume of 120  $\mu$ l and vortexed for 5 sec. The growth medium was removed from the wells, and cells were rinsed with DPBS (150  $\mu$ l). Serum-free medium (no phenol red, 120  $\mu$ l) was added to the wells, followed by aliquots of polymer dilutions (30  $\mu$ l). The final polymer concentration in the wells were 0, 1, 2.5, 5, 7.5, 10, 15, 20, 30, 40, 60, 100 and 150  $\mu$ g/ml. Plates were incubated at 37°C and 5% CO<sub>2</sub> for 4 h, after which the medium in each well was replaced with fresh growth medium (DMEM with 10% *v/v* FBS, 150  $\mu$ l). Plates were incubated at 37°C and 5% CO<sub>2</sub> for an additional 44 h. Cytotoxicity was assessed by the MTS Assay using CellTiter 96® AQueous One Solution Cell Proliferation Assay (Promega, Madison WI) according to the manufacturer's instructions. Following incubation of the plates at 37°C and 5% CO<sub>2</sub> for 2 h, the absorbance was read at  $\lambda_{\text{abs}}$ =490 nm. Data was fitted to sigmoidal (dose-response) curve using OriginPro 8.1, and the half maximal inhibitory concentrations (IC<sub>50</sub>) were calculated as the polymer concentration (in  $\mu$ g/ml) corresponding to 50% cell survival or half the absorbance measured at a polymer concentration of 0  $\mu$ g/ml. Each condition was performed in triplicate.

### siRNA Transfection

MDA-MB-231-luc+ (8,000 cells/well) were seeded in 100  $\mu$ l of growth medium (DMEM with 10% *v/v* FBS) in both white and clear 96-well polystyrene plates (tissue-culture treated) 24 h prior to transfection and incubated at 37°C and 5% CO<sub>2</sub>. Immediately prior to transfection, polyplexes were formed as previously described. The growth medium



was removed from the wells, and cells were rinsed with DPBS (150  $\mu$ l). Serum-free medium (no phenol red, 120  $\mu$ l) was added to the wells, followed by aliquots of the polyplex solution (30  $\mu$ l). The siRNA concentration per well was varied from 0.33  $\mu$ g/ml (50 ng of siRNA/well) to 3  $\mu$ g/ml (450 ng of siRNA/well). Plates were incubated at 37°C and 5% CO<sub>2</sub> for 4 h, after which the medium in each well was replaced with fresh growth medium (DMEM with 10% *v/v* FBS, 150  $\mu$ l). Plates were incubated at 37°C and 5% CO<sub>2</sub> for an additional 44 h.

As positive controls, cells were transfected with PEIb, RNAiFECT (Qiagen) and TransIT-siQuest (Mirus Bio, Madison WI). Transfections with PEIb followed the same procedure as previously described for polymer conjugates. Complex formation with RNAiFECT was performed according to the manufacturer's instructions with a siRNA:RNAiFECT ( $\mu$ g: $\mu$ l) = 1:6 in the Buffer EC-R supplied. Complex formation with TransIT-siQuest was performed according to the manufacturer's instructions with a siRNA:RNAiFECT ( $\mu$ g: $\mu$ l) = 1:5 in Opti-MEM. The growth medium was removed from the wells, and cells were rinsed with DPBS (150  $\mu$ l). Serum-free medium (no phenol red, 120  $\mu$ l) was added to the wells, followed by aliquots of the complex solution (30  $\mu$ l). Plates were incubated at 37°C and 5% CO<sub>2</sub> for 4 h, after which the medium in each well was replaced with fresh growth medium (DMEM with 10% *v/v* FBS, 150  $\mu$ l). Plates were incubated at 37°C and 5% CO<sub>2</sub> for an additional 44 h.

White 96-well plates were assayed for luciferase activity using Bright-Glo Luciferase Assay (Promega, Madison WI) according to the manufacturer's instructions. Clear 96-well plates were assayed for either total protein content using BCA Protein Quantification Assay (Thermo Scientific Pierce) according to the manufacturer's instructions or relative cell viability by MTS assay as previously described. Each polyplex/control condition was performed in triplicate for luciferase activity, total protein quantification and cell viability.

### Bright-Glo Luciferase Assay

Prior to luciferase activity quantification, growth medium was removed from the wells of the white 96-well plate, and cells were rinsed with DPBS (150  $\mu$ l). Serum-free medium (no phenol red, 100  $\mu$ l) was added to each well. Bright-Glo working solution (Promega, Madison WI; 100  $\mu$ l) was added to each well. The plate was incubated for 2 min at room temperature, and luminescence (in RLU units) was immediately obtained.

### BCA Protein Quantification Assay

Prior to total protein quantification, growth medium was removed from the wells of the clear 96-well plate, and

cells were rinsed with DPBS (150  $\mu$ l). Glo-lysis buffer (Promega, Madison WI; 10  $\mu$ l) was added to each well, and plates were gently shaken at room temperature on a microplate shaker for 10 min. BCA working solution (Thermo Scientific; 200  $\mu$ l) was added to each well and incubated at 37°C and 5% CO<sub>2</sub> for 1 h. Absorbance was read at  $\lambda_{\text{abs}}$ =562 nm. The total protein (in  $\mu$ g/well) was calculated from a calibration curve generated from a BSA protein standard with concentrations varying from 0 to 2000  $\mu$ g/ml performed simultaneously with each experiment.

### Statistical Analysis

All data included is presented as the mean  $\pm$  standard deviation. Statistical analysis between samples was performed via a two-tailed unpaired t-test. Difference between samples were considered significant if  $p < 0.05$ .

## RESULTS

### Polymer Conjugates

pAA was synthesized via RAFT polymerization using A-CPA and CPA-DB as the radical initiator and chain transfer agent (CTA), respectively. By varying the monomer to CTA molar ratio, pAA of four different  $M_n$ , specifically 2,900 kDa, 4,800 kDa, 10,400 kDa and 20,900 kDa, were synthesized with PDIs ranging from 1.36 to 1.19 depending on the  $M_n$ . The  $M_n$  range for pAA was selected based on the limited solubility of the polymer conjugates with the highest molecular weight at physiological pH of 7.4.

A library of polymers was synthesized by conjugating two distinct moieties, Agm and Gal, at different ratios to the side chains of pAA. The conjugation of both moieties was mediated via an amidation reaction between the side chain carboxyl groups in pAA and the amino groups in the ligands using DMTMM as the condensing agent (18). The conjugation of both ligands to pAA was achieved in a two-step reaction, where Agm was first introduced followed by Gal (Fig. 1). Simultaneous conjugation of both ligands is possible; however, in order to achieve high Agm content (>39%), a two-step conjugation reaction was required. The degree of side chain substitution of each ligand was determined by <sup>1</sup>H NMR spectroscopy (Inova 400 MHz, D<sub>2</sub>O) and is referred to as a percentage value. The percentage reported (mol %) corresponds to the total ligand content relative to the total side chains (or repeating units) in each polymer. To obtain different ligand content, the [COOH]<sub>0</sub> to [DMTMM]<sub>0</sub> molar ratio was varied while keeping [NH<sub>2</sub>]<sub>0</sub> = 2·[DMTMM]<sub>0</sub> and [polymer]<sub>0</sub> = 3.0 mg/ml. Of note,

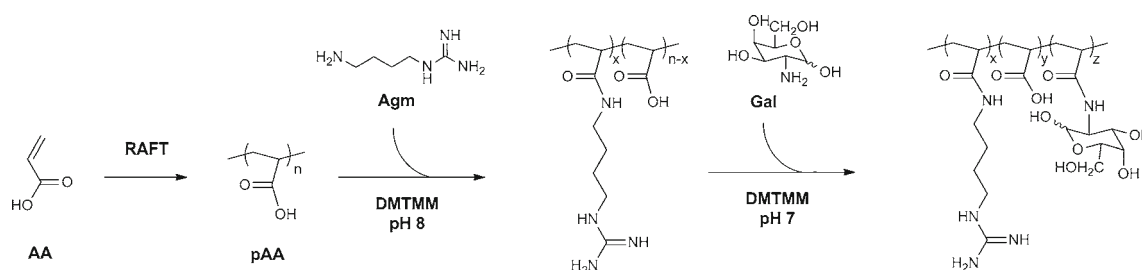


**Fig. 1** Synthesis schematic of polymer conjugates. Polymers precursors (pAA) were synthesized by RAFT polymerization with different molecular weights followed by a two-step conjugation of Agm and Gal at different mol percent (%) substitutions.

partial methylation of the carboxyl side chain group (~6%) occurred during synthesis of the polymer precursor. This modification produced a  $^1\text{H}$  NMR signal at 3.7 ppm (s, 3H), which was accounted for the quantitation of Gal substitution in pAA.

Table I outlines the polymer conjugates comprising the library with their corresponding  $M_n$ , PDI, Gal content and Agm content. A total of 22 polymers were evaluated; four pAA  $M_n$ , and six polymer conjugates (except for 21 kDa-P polymers) per polymer  $M_n$ , each with a unique combination of Agm and Gal content. For the 21 kDa-P library, only four Gal/Agm combinations (21-P1 to 21-P4) were included due to poor solubility at physiological pH of 7.4 for the 21-P5 and 21-P6 polymers.

### Relative Binding Affinity

Figure 2a–d shows the relative binding affinity of the polymer conjugates with siRNA at various polymer:siRNA (w:w) ratios: (a) 3 kDa-P, (b) 5 kDa-P, (c) 10 kDa-P and (d) 21 kDa-P. The relative strength of the electrostatic interactions between the polymer chains and siRNA can be measured by EtBr fluorescence quenching. EtBr intercalates between the strands of nucleic acids generating a strong fluorescence signal. Maintaining the siRNA concentration constant, as the polymer concentration in solution increases, the EtBr will be excluded from interacting with the siRNA, thereby generating a reduction in the fluorescence signal. This quenching effect provides a quantitative analysis of the relative binding affinity of the polymer conjugates with siRNA (20). In Fig. 2, a relative fluorescence of 1 (highest possible value) corresponds to free siRNA in solution (no binding to polymer); therefore, the lower the relative fluorescence, the stronger the binding affinity of the polymer with siRNA.

From Fig. 2a–d a trend directly correlated to the Agm and Gal contents can be distinguished for all polymers conjugates. The higher the Agm content, the higher the cationic density in the polymer chain leading to a stronger electrostatic interaction with the negatively charged siRNA.

The Gal content in the polymer influences the total cationic density as well through its conjugation to the free carboxyl groups in pAA which, if unconjugated, would become ionized in solution imparting a more negative charge. Therefore, keeping the Agm content constant, the higher the Gal content the more effective the binding of the polymer conjugate with siRNA.

For all molecular weights, P1 and P2 polymers had higher affinities for siRNA resulting in a relative fluorescence of ~0.2 at a polymer:siRNA (w:w)  $\geq 5:1$  or higher. The low level of fluorescence correlates to a strong binding affinity between these polymers and siRNA. As the Agm content decreases, the binding affinity to siRNA decreases. For instance, P3 and P4 polymers generated a relative fluorescence of ~0.3–0.4 at a polymer:siRNA (w:w)  $\geq 20:1$  for 3 kDa-P and 5 kDa-P, and at a polymer:siRNA (w:w)  $\geq 10:1$  for 10 kDa-P and 21 kDa-P. For P5 polymers the relative fluorescence decreased to ~0.4–0.5; however, to achieve this a polymer:siRNA (w:w) ratio of 40:1 or higher is required. P6 polymers generate a relative fluorescence of ~0.6–0.8 at a polymer:siRNA (w:w)  $\geq 20:1$ .

### Heparin Competitive Displacement

To evaluate the polyplex stability in the presence of other anionic compounds, a heparin competitive displacement assay was carried out. In this assay, the polyplex is exposed to varying amounts of heparin, a highly anionic polysaccharide. Heparin competes with the siRNA for interactions with the polymer conjugate, thereby displacing the siRNA from the complex. This dissociation can be evaluated by quantifying the displaced siRNA in solution by means of EtBr fluorescence. A relative polyplex stability (RPS) is calculated from Eq. 1:

$$RPS = \frac{F_{siRNA} - F_{hep}}{F_{siRNA} - F_{polyplex}} \quad (1)$$

where  $F_{siRNA}$  is the corrected fluorescence of siRNA in the absence of the polymer vector,  $F_{polyplex}$  is the corrected

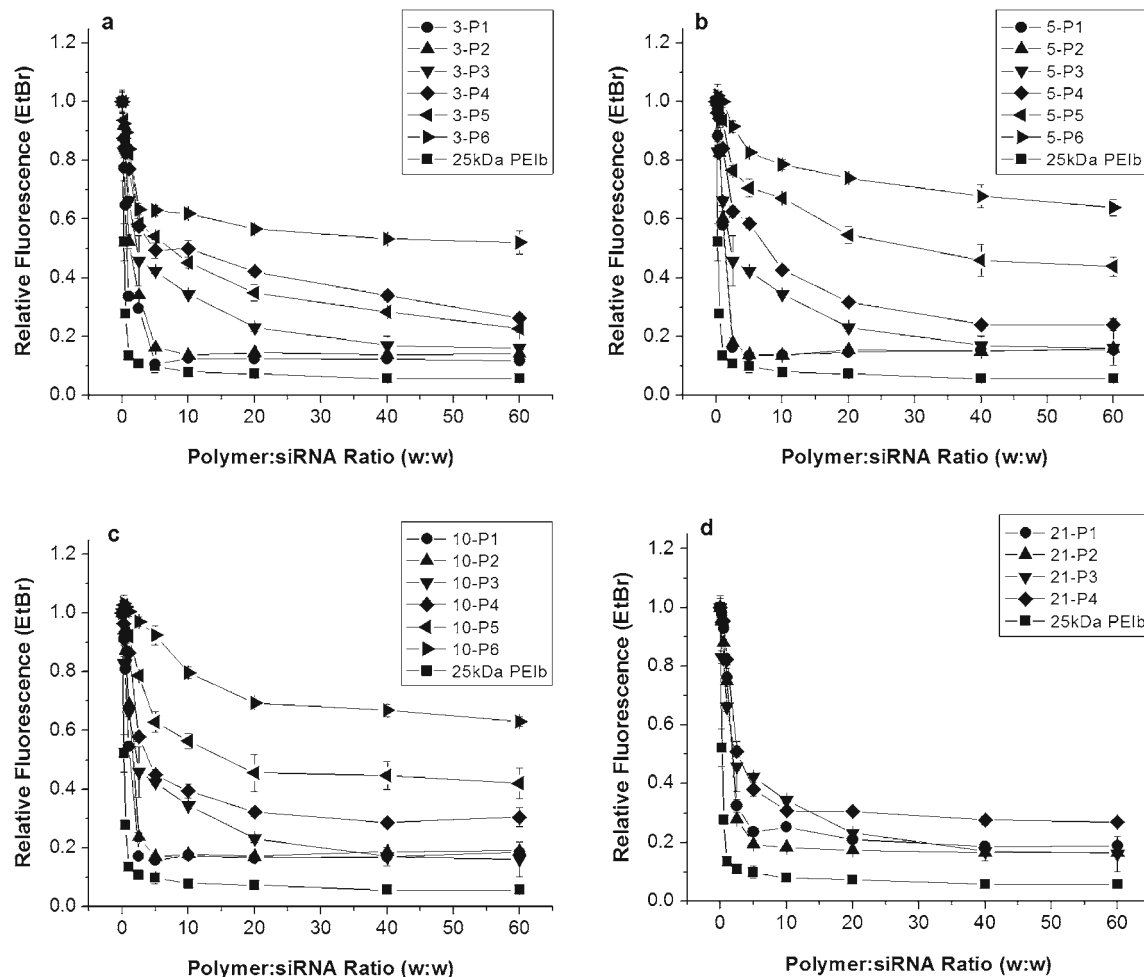


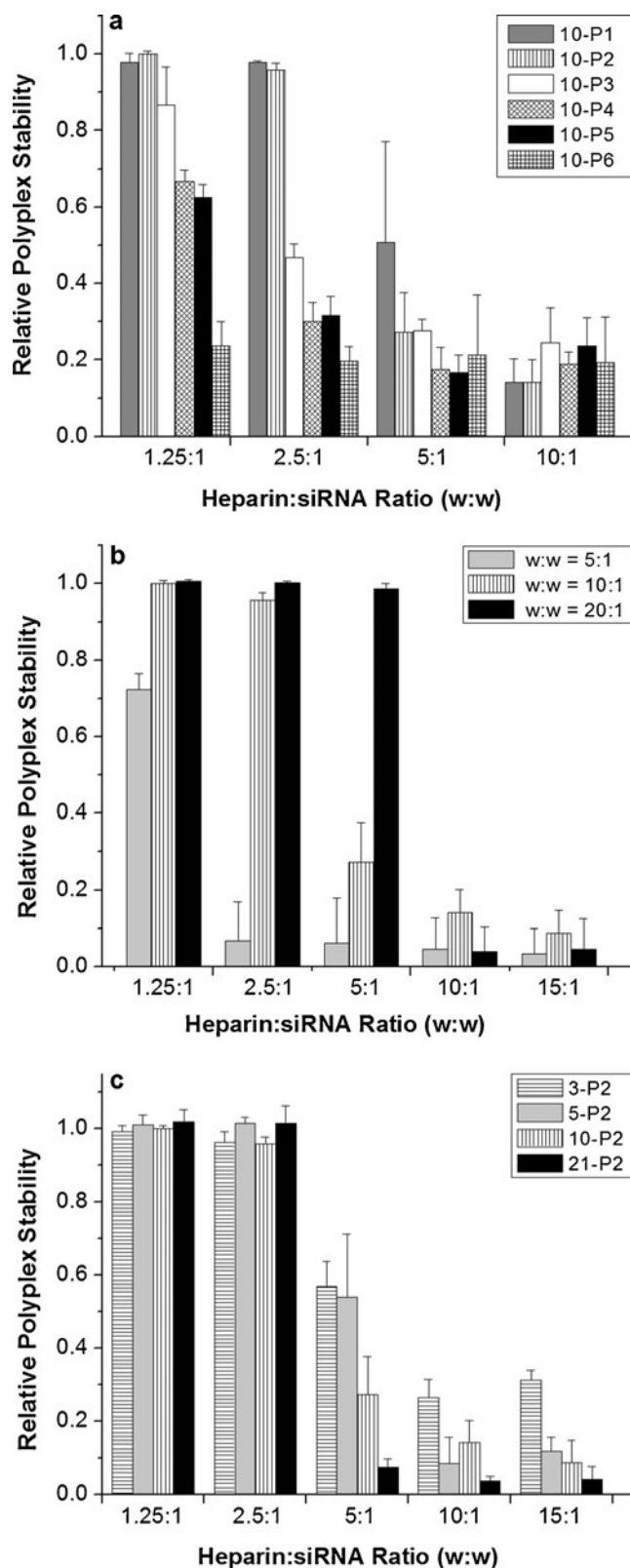
**Fig. 2** Relative binding affinity of polymer conjugates with siRNA as measured by ethidium bromide fluorescence quenching. [siRNA]=3  $\mu$ g/ml.  $N=3$ . Error bars represents standard deviation. 25 kDa PEIb is included for comparison. (a) 3 kDa-P; (b) 5 kDa-P; (c) 10 kDa-P; (d) 21 kDa-P.

fluorescence of siRNA in the presence of the polymer conjugate and  $F_{hep}$  is the corrected fluorescence of siRNA in the presence of the polymer conjugate and heparin.  $RPS=1$  corresponds to [heparin]=0  $\mu$ g/ml, or when the fluorescence emitted from the system with heparin ( $F_{hep}$ ) is equal to the fluorescence emitted from the system without heparin ( $F_{polyplex}$ ). A lack of change in fluorescence corresponds to no additional siRNA:polymer dissociation due to heparin, which correlates to high stability. Therefore, the higher the RPS value (the closer to 1), the more stable the polyplexes in the presence of heparin. Figure 3a–c shows the RPS after exposing the polyplex to varying amounts of heparin. Taking the 10 kDa-P library as a representative example (Fig. 3a), polymers with higher Agm content, particularly 10-P1 and 10-P2, provide a stronger resistance to exchange with heparin, which correlates to a stronger binding affinity with siRNA. Taking 10-P2 as a representative example, as the polymer:siRNA (w:w) ratio increases, the strength of electrostatic binding between

siRNA and the polymer increases, thus higher amounts of heparin are needed to disrupt the siRNA-polymer complex (Fig. 3b). For instance heparin:siRNA (w:w) = 2.5:1 is required to disrupt a polymer:siRNA (w:w) = 5:1, while a heparin:siRNA (w:w) = 5:1 is required to disrupt a polymer:siRNA (w:w) = 10:1 and a heparin:siRNA (w:w) = 10:1 is required to disrupt a polymer:siRNA (w:w) = 20:1. The polymer  $M_n$  also has an impact on the RPS by the competitive binding of heparin. It is evident from Fig. 3c that lower  $M_n$  polymers provide higher polyplex

**Fig. 3** Relative polyplex stability. Displacement of siRNA from polyplex by the competitive interaction of heparin with polymer conjugates was measured by ethidium bromide fluorescence quenching. [siRNA]=3  $\mu$ g/ml.  $N=3$ . Error bars represent standard deviation. (a) 10 kDa-P library at polymer:siRNA (w:w) = 10:1: 10-P1 (dark gray), 10-P2 (vertical lines), 10-P3 (white), 10-P4 (diamond), 10-P5 (black), 10-P6 (squares). (b) 10-P2 at various polymer:siRNA (w:w) ratios: w:w=5:1 (light gray), w:w=10:1 (vertical lines) and w:w=20:1 (black). (c) P2 polymers at polymer:siRNA (w:w)=10:1: 3-P2 (horizontal lines), 5-P2 (light gray), 10-P2 (vertical lines), 21-P2 (black).





stability in solution as it shows less siRNA displacement by competitive anionic species as compared to their higher  $M_n$  counterparts.

### Polyplex Stability in Serum

The polyplex stability in serum, and the ability of the polymer conjugate to protect the siRNA from nuclease degradation, was evaluated. In this assay, polyplexes were incubated in 10% FBS for various times, after which the integrity of the siRNA was examined via gel electrophoresis. Figure 4 shows images of RNA polyacrylamide gels with each lane corresponding to a different incubation time. Naked siRNA was degraded within 2 h of incubation in 10% FBS (Fig. 4a), while siRNA recovered from polyplexes formed with 10-P2 and 10-P3 remained almost intact at 48 h and 16 h of incubation in 10% FBS, respectively (Fig. 4b–c). These data suggest that the selected polymer conjugates are able to protect the siRNA from serum nuclease degradation.

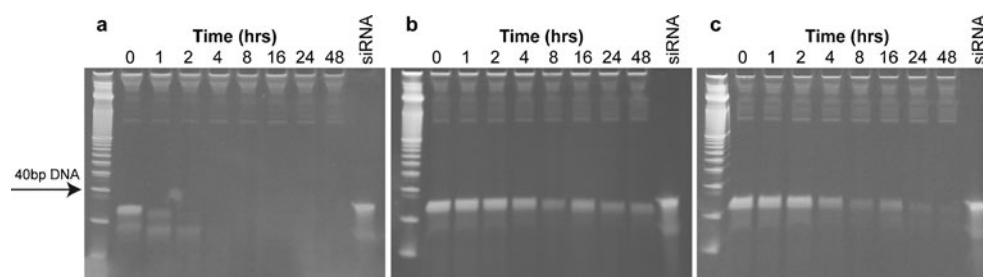
### Effective Diameter and Zeta Potential

Figure 5 shows the effective diameter of polyplexes formed from the polymer conjugates and siRNA at a polymer:siRNA (w:w) = 10:1. For all molecular weights, a trend was distinguished where particle size increases as  $Ag_m$  content decreases. For the 10 kDa-P library at a polymer:siRNA (w:w) = 10:1, the particle size ranges from 125 nm to 180 nm. Decreasing, as well as increasing, the polymer  $M_n$  showed a decrease in effective diameter reaching particle sizes of ~80 nm. In addition, particularly for 10-P2, increasing the polymer:siRNA (w:w) ratio to 20:1 decreases the particle size to ~90 nm (Supplementary Figure S1). Similar trends were observed for other molecular weights.

Figure 6 shows the zeta potential of polyplexes formed from the polymer conjugates and siRNA at a polymer:siRNA (w:w) = 10:1. All polymers conjugates, except the P6 polymers, achieved polyplexes that exhibited positive zeta potentials ranging from 20 to 40 mV. Polyplexes formed from P6 polymers had net negative zeta potentials. Taking 10-P2 as a representative example at varying polymer:siRNA (w:w) of 1:1, 2.5:1, 5:1, 10:1 and 20:1, polyplexes exhibit net positive zeta potentials of similar values except for polymer:siRNA (w:w) = 1:1, which had a negative zeta potential (Supplementary Figure S2).

### Confocal Microscopy

Confocal microscopy imaging was performed to visualize the internalization of polyplexes into MDA-MB-231-luc+ cells. Two FA-labeled polymer conjugates, 10-P2-FA and 10-P3-FA, were selected as representative examples for this analysis due to their high cationic charge and relative good polyplex stability. For both conjugates, polyplex internalization was achieved as distinguished by the strong fluorescence emitted from the interior of the cell 4 h post-transfection



**Fig. 4** Polyplex stability in serum. siRNA integrity was evaluated by gel electrophoresis after incubation of polyplexes at 37°C in 10% v/v FBS at various times. siRNA bands were stained with SYBR green II RNA gel stain and visualized under a UV transilluminator. Lane 1 corresponds to a 10 bp DNA ladder. (a) naked siRNA; (b) polyplexes formed with 10-P2 and siRNA (polymer:siRNA (w:w)=10:1); (c) polyplexes formed with 10-P3 and siRNA (polymer:siRNA (w:w)=20:1).

(Fig. 7). Punctuated as well as diffused fluorescence was observed in both samples.

### Cytotoxicity

The cytotoxicity caused by free polymer conjugates was assessed by calculating their  $IC_{50}$ , which corresponds to the polymer concentration required to kill 50% of the cell population. A sigmoidal fit was applied to the plot of  $\log_{10}(\text{polymer concentration})$  vs. relative absorbance at 490 nm (MTS assay), and the polymer concentration was calculated at 50% cell survival.

Table II includes the  $IC_{50}$  of all polymer conjugates. Two trends are distinguished for these polymer conjugates: 1) the cytotoxicity decreases as Agm content decreases; 2) the cytotoxicity decreases as polymer  $M_n$  decreases. Polymer-induced cytotoxicity was more prominent for P1 and P2 polymers, which had conserved  $IC_{50}$  of ~5–6  $\mu\text{g/ml}$  for all

molecular weights. Nevertheless, for all polymer conjugates, the cytotoxicity obtained was lower than for 25 kDa PEIb, which had an  $IC_{50}$ =2.9  $\mu\text{g/ml}$  under the same conditions.

### siRNA Transfection

MDA-MB-231-luc+ cells were transfected with siRNA targeting the luciferase protein. Figure 8a–d shows the relative cell viability and relative luciferase expression 48 h after siRNA transfection mediated by polymer conjugates. Polyplexes were formed at various polymer:siRNA (w:w) ratios with a constant siRNA concentration of 0.33  $\mu\text{g/ml}$  (50 ng/well). Luciferase expression (RLU) was normalized to the total protein content as determined by the BCA total protein assay. Cell viability 48 h post-transfection was quantified using the MTS assay.

A wide range of polymer:siRNA (w:w) ratios for each polymer conjugate was assessed to identify optimal parameters that would achieve the highest transfection efficiency. For each polymer conjugate, the polymer:siRNA (w:w) ratio

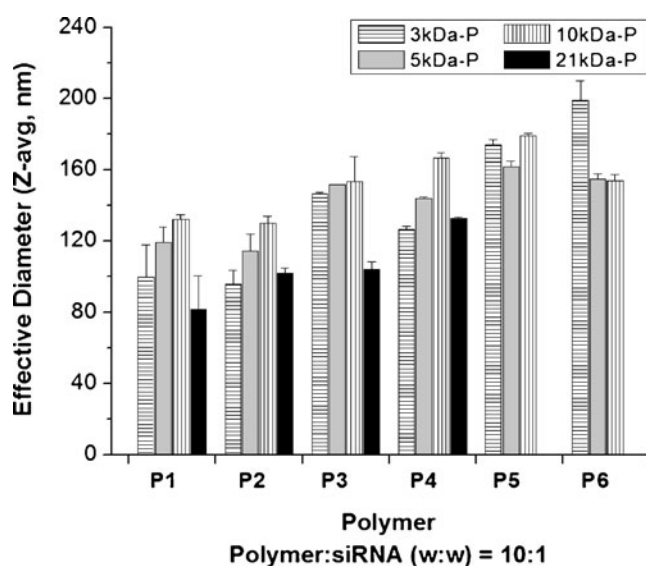


**Fig. 5** Effective diameter (Z-ave, nm) of polyplexes formed from siRNA and polymer conjugates at a polymer:siRNA (w:w)=10:1: 3 kDa-P (horizontal lines), 5 kDa-P (dark gray), 10 kDa-P (vertical lines), 21 kDa-P (black). [siRNA]=5  $\mu\text{g/ml}$ . Three measurements were performed on each sample. Error bars represents standard deviation.

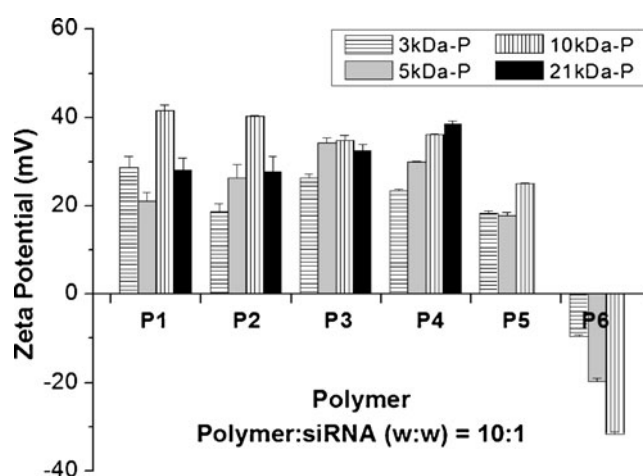
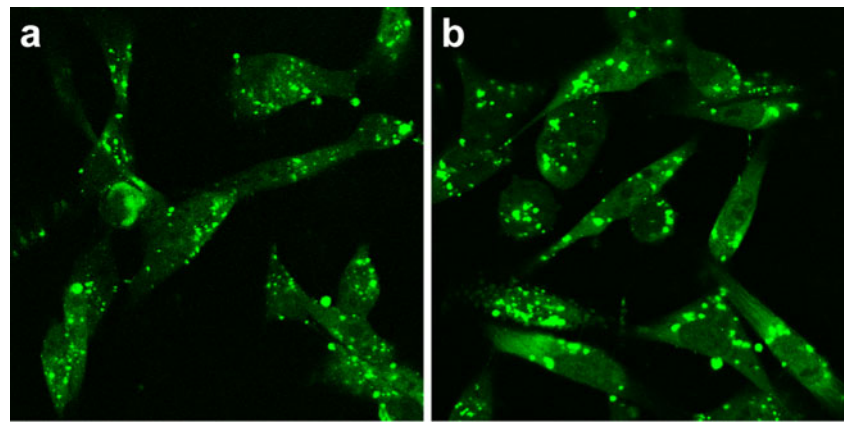


**Fig. 6** Zeta potential (mV) of polyplexes formed from siRNA and polymer conjugates at a polymer:siRNA (w:w)=10:1: 3 kDa-P (horizontal lines), 5 kDa-P (dark gray), 10 kDa-P (vertical lines), 21 kDa-P (black). [siRNA]=5  $\mu\text{g/ml}$ . Three measurements were performed on each sample. Error bars represents standard deviation.

**Fig. 7** Confocal microscopy images of polyplexes internalized by MDA-MB-231-luc+ cells 4 h post-transfection. Cells were transfected with polyplexes formed from FA-labeled polymer conjugates and siRNA. [siRNA] = 0.67  $\mu$ g/ml (1.5  $\mu$ g siRNA per plate). **(a)** 10-P2-FA, polymer:siRNA (w:w) = 10:1; **(b)** 10-P3-FA, polymer:siRNA (w:w) = 20:1.



was varied according to their relative binding affinities with siRNA and to IC<sub>50</sub> values. For all molecular weights, polymers with the highest Agm content, particularly P1, P2 and P3 polymers, achieved enhanced transfection efficiency as compared to those with low Agm content, leading to a lower protein expression 48 h after treatment.

Although no detectable cytotoxicity was perceived for the 3 kDa-P library at a constant siRNA concentration of 0.33  $\mu$ g/ml, only a modest protein knockdown of ~40%

**Table II** IC<sub>50</sub> Values for Polymer Conjugates and 25 kDa PEIb after 48 h Incubation with MDA-MB-231-Luc Cells + (MTS assay). N=3

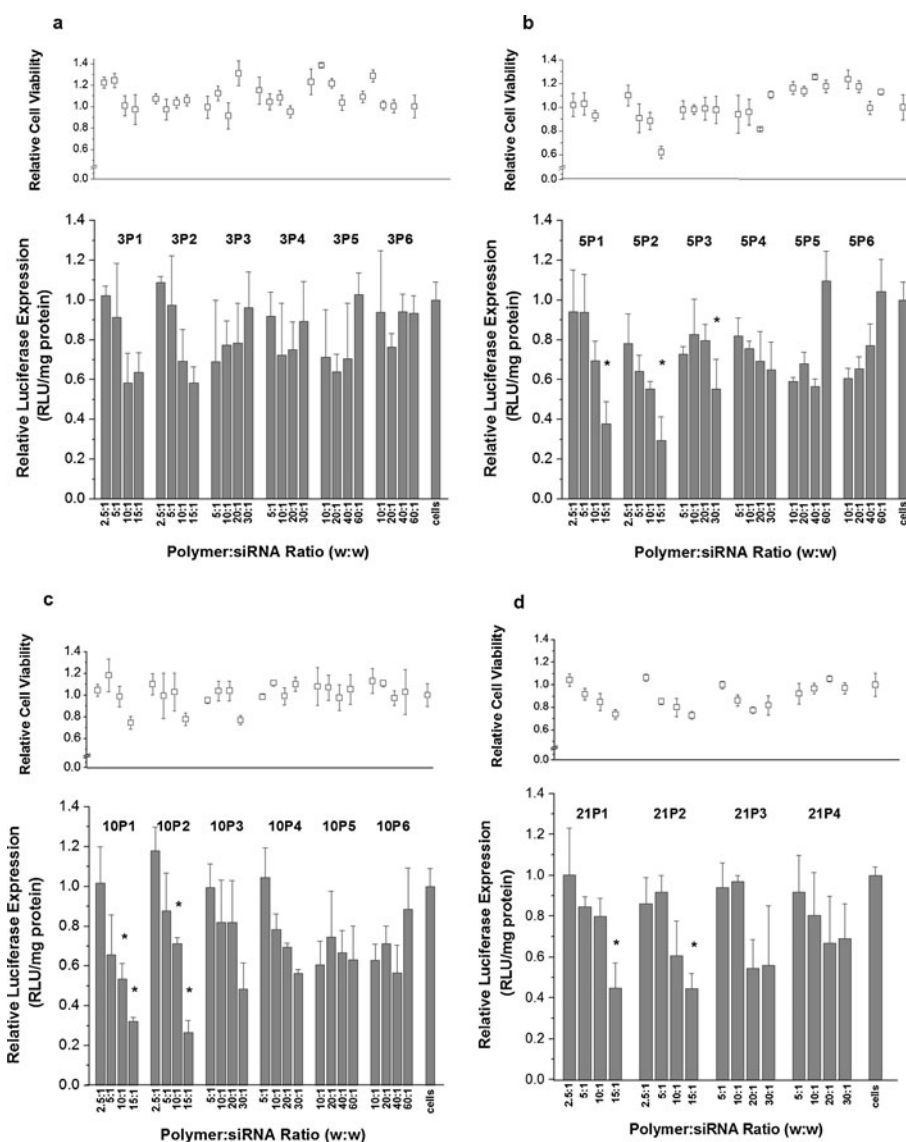
Entry	Polymer	IC <sub>50</sub> , free polymer ( $\mu$ g/ml)
1	3-P1 3kDapAA-76%A	6.5 $\pm$ 0.2
2	3-P2 3kDapAA-76%A-3%G	7.5 $\pm$ 0.7
3	3-P3 3kDapAA-56%A-17%G	55.7 $\pm$ 1.9
4	3-P4 3kDapAA-56%A-8%G	121.9 $\pm$ 2.5
5	3-P5 3kDapAA-45%A-22%G	> 150
6	3-P6 3kDapAA-45%A-13%G	> 150
7	5-P1 5kDapAA-76%A	5.0 $\pm$ 0.5
8	5-P2 5kDapAA-76%A-2%G	5.2 $\pm$ 0.7
9	5-P3 5kDapAA-55%A-17%G	54.9 $\pm$ 1.1
10	5-P4 5kDapAA-55%A-10%G	48.8 $\pm$ 1.2
11	5-P5 5kDapAA-46%A-28%G	> 150
12	5-P6 5kDapAA-46%A-14%G	> 150
13	10-P1 10kDapAA-78%A	4.7 $\pm$ 0.4
14	10-P2 10kDapAA-78%A-3%G	5.9 $\pm$ 0.4
15	10-P3 10kDapAA-56%A-18%G	13.1 $\pm$ 0.9
16	10-P4 10kDapAA-56%A-10%G	20.2 $\pm$ 1.0
17	10-P5 10kDapAA-46%A-26%G	> 150
18	10-P6 10kDapAA-46%A-14%G	> 150
19	21-P1 10kDapAA-72%A	6.5 $\pm$ 0.6
20	21-P2 10kDapAA-72%A-3%G	5.4 $\pm$ 0.5
21	21-P3 10kDapAA-55%A-12%G	10.0 $\pm$ 0.9
22	21-P4 10kDapAA-55%A-4%G	15.3 $\pm$ 0.6
23	PEIb 25 kDa	2.9 $\pm$ 0.3

was achieved with 3-P1 and 3-P2 polymers at various polymer:siRNA (w:w) ratios. However, these values are not statistically significant compared to non-specific siRNA transfection carried out under the same conditions. In contrast, 5 kDa-P and 10 kDa-P libraries were both more successful at siRNA transfection and protein knockdown compared to the 3 kDa-P library, particularly for P1 and P2 polymers. 5-P1 and 5-P2 at a polymer:siRNA (w:w) = 15:1 achieved ~60% knockdown while 10-P1 and 10-P2 at a polymer:siRNA (w:w) = 15:1 achieved ~70% knockdown, all being statistically significant compared to non-specific siRNA transfection carried out under the same conditions ( $p < 0.05$ ). In addition, for both libraries, P3 polymers at a polymer:siRNA (w:w) = 30:1 achieve ~40–50% protein knockdown. As the Agm content was decreased, less significant knockdown was observed (~0–40% protein knockdown). In the case of the 21 kDa-P library, only 21-P1 and 21-P2 at a polymer:siRNA (w:w) = 15:1 showed protein knockdown that was statistically significant as compared to non-specific siRNA transfection carried out under the same conditions ( $p < 0.05$ ). Under these conditions, protein knockdown of ~56% was achieved with a relative cell viability >70%.

Polymer conjugates that exhibited negligible cytotoxicity, though modest transfection efficiencies at siRNA concentration of 0.33  $\mu$ g/ml, were further evaluated for protein knockdown at higher siRNA concentrations up to 3.0  $\mu$ g/ml (Fig. 9a–d). These polymer conjugates include P3 polymers at a polymer:siRNA (w:w) = 10:1 and polymer:siRNA (w:w) = 20:1, and P5 polymers at polymer:siRNA (w:w) = 60:1. For all conditions, increasing the siRNA concentration led to a significant increase in protein knockdown. P3 polymers at a polymer:siRNA (w:w) = 20:1 were shown to be the most effective transfection reagents as revealed by the marked decrease in relative luciferase expression. Particularly, 5-P3 polymers at polymer:siRNA (w:w) = 20:1 achieved up to 84% protein knockdown with >70% cell viability.

Transfection of siRNA with 25 kDa PEIb and two commercially-available transfection reagents (RNAiFECT

**Fig. 8** Relative cell viability and relative luciferase expression of MDA-MB-231-luc+ cells 48 h post-transfection for all polymer conjugates at [siRNA]=0.33  $\mu$ g/ml (50 ng siRNA/well).  $N=3$ . Error bars represent standard deviation. Conditions showing statistically significant protein knockdown ( $p < 0.05$ ) as compared to nonspecific siRNA transfection carried out under the same conditions are indicated by an asterisks (\*). (a) 3 kDa-P; (b) 5 kDa-P; (c) 10 kDa-P; and (d) 21 kDa-P.



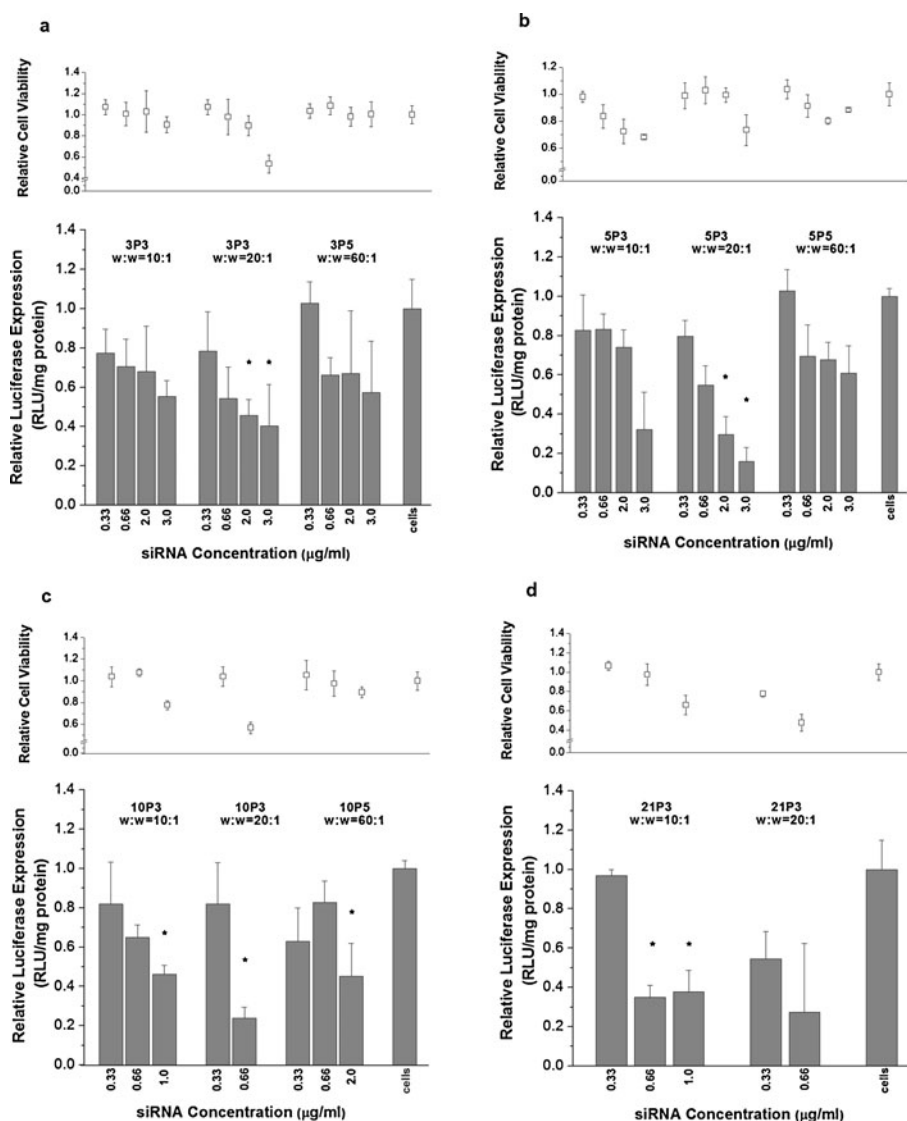
and TransIT-siQuest) were included for comparison (Fig. 10). Some of the conditions evaluated for our polymer conjugates achieved better outcomes than PEIb which could generate up to ~55% protein knockdown at [siRNA] = 0.33  $\mu$ g/ml (PEIb:siRNA (w:w) = 5:1) or [siRNA] = 0.66  $\mu$ g/ml (PEIb:siRNA (w:w) = 2.5:1). Higher siRNA concentrations or PEIb:siRNA (w:w) ratios to enhance protein knockdown is not viable due to the high cytotoxicity caused by PEIb. For the commercially-available transfection reagents, at analogous conditions, protein knockdown of ~60% and ~80% was achieved for RNAiFECT and TransIT-siQuest, respectively. As controls, relative luciferase expression of MDA-MB-231-luc+ cells 48 h post-transfection with non-specific siRNA and with polymer conjugates only (no siRNA) for polymer conjugates were evaluated and a selection are shown in Supplementary Figure S3 and Figure S4.

## DISCUSSION

The favorable transfection of siRNA into cultured cells is reliant on multiple factors including the structural components of the vector and the vector:siRNA ratio. These features alter both the biophysical and biochemical properties of the vector and can influence siRNA delivery efficiency. Herein we have analyzed a library of pAA-based polymer conjugates with a variety of structural elements including varying polymer  $M_n$ , side chain composition and side chain density. One of the major advantages of pAA scaffolds is the availability of multiple sites that can easily undergo chemical modification by following an aqueous-based, easy to purify, one-step condensation reaction. Although we only show the conjugation of two ligands, this class of material offers the potential for multiple combinations of different functional groups following a similar chemistry.



**Fig. 9** Relative cell viability and relative luciferase expression of MDA-MB-231-luc+ cells 48 h post-transfection with varying siRNA concentration. Polymers evaluated were P3 (polymer: siRNA (w:w)=10:1) and polymer: siRNA (w:w)=20:1 and P5 (polymer: siRNA (w:w)=60:1) polymers.  $N=3$ . Error bars represent standard deviation. Conditions showing statistically significant protein knockdown ( $p < 0.05$ ) as compared to non-specific siRNA transfection carried out under the same conditions are indicated by an asterisks (\*). (a) 3 kDa-P; (b) 5 kDa-P; (c) 10 kDa-P; and (d) 21 kDa-P



One of the side chain functional groups incorporated into the design is agmatine (Agm), which imparts a cationic density essential for electrostatic interactions between the polymer chains and siRNA, as well as the cellular membrane. The guanidium groups from the Agm moieties are protonated under physiological conditions providing a strong electrostatic interaction with negatively charged phosphate groups along the siRNA backbone. Moreover, Agm has been shown to promote cellular internalization due to interactions between the guanidium groups and the sulfate groups of the cell surface glycosaminoglycan (21). The number of guanidium groups in arginine-rich peptides has been found to significantly influence translocation (22,23). Thus controlling the Agm content is critical for efficient interactions with the cell membrane. The second component incorporated into the design is D-(+)-galactosamine (Gal). Carbohydrates can enhance transfection efficiencies and, in this case, the hydroxyl groups in Gal help stabilize the cationic charge from the Agm

groups and therefore increase the polymer solubility. In addition, although not evaluated in this study, carbohydrates could potentially promote cell-specific targeting through lectins (sugar-binding proteins) localized on the membranes of specific cells, such as hepatocytes (24–29). However, the degree of substitution of Gal into polymer vectors can have an impact on the polyplex size and transfection efficiency (25). Therefore, careful identification of optimal number of Gal residues in the polymer is crucial for effective siRNA delivery.

The library contains a total of 22 polymers; four polymer precursors of distinct  $M_n$  (3 kDa, 5 kDa, 10 kDa to 21 kDa), each with varying combinations of Agm and Gal content. The higher the Agm content in the polymer, the stronger electrostatic binding with siRNA and the higher polyplex stability in the presence of other anionic species, in addition to smaller effective particle diameters and higher net zeta potentials. However, polymer conjugates with high Agm content generate higher cytotoxicity as identified by their low  $IC_{50}$  ( $\sim 5 \mu\text{g/ml}$ ).



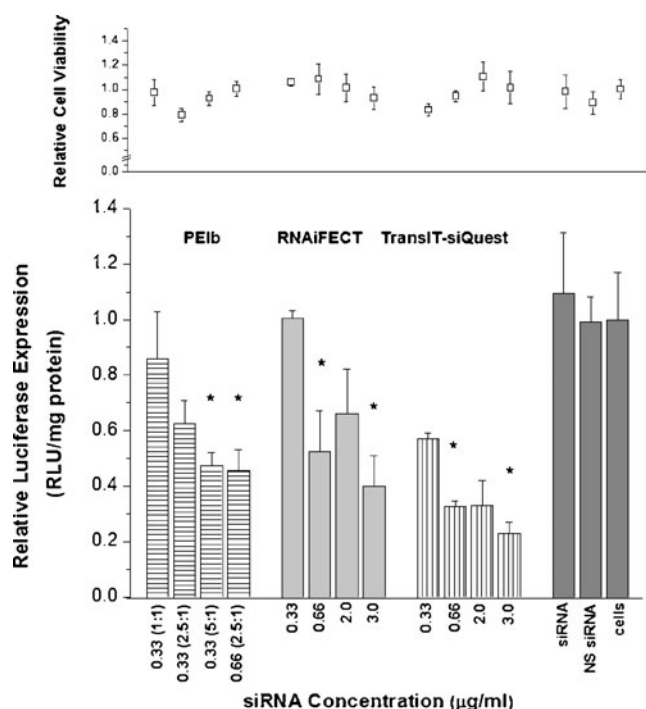


**Fig. 10** Relative cell viability and relative luciferase expression of MDA-MB-231-luc+ cells 48 h post-transfection. Commercially-available transfection reagents: 25 kDa PEIb (horizontal lines), RNAiFECT (light gray), TransIT-siQuest (vertical lines), siRNA (3.0 µg/ml), non-specific (NS) siRNA (3.0 µg/ml) and cells only (dark gray).  $N=3$ . Error bars represent standard deviations. Conditions showing statistically significant protein knockdown ( $p < 0.05$ ) as compared to nonspecific siRNA transfection carried out under the same conditions are indicated by an asterisks (\*).

In contrast, polymers with the lowest amount of Agm (45%–46%) exhibited minimal cytotoxicity ( $IC_{50} > 150 \mu\text{g/ml}$ ); however these have a lower binding affinity with siRNA. This phenomenon may be due to the low amount of guanidium groups and the presence of both positive and negative charges in the polymer chain, which may hinder the siRNA to effectively interact with available positive charges. The polymer  $M_n$  influences the biophysical properties of these vectors, particularly the stability in the presence of anionic species. Polymers with lower  $M_n$  are more stable in the presence of heparin than their higher  $M_n$  counterparts, likely due to their more comparable chain length with siRNA. Polycations and polyanions with charged segments of matched chain length have been found to undergo molecular recognition in solution forming assemblies of higher stability (30). In addition, for P2 polymers, effective diameters of less than 100 nm and high binding affinity with siRNA correlated to higher protein knockdown. However, comparing polymer conjugates with the same polymer:siRNA (w:w) ratio of 10:1, no apparent structure-function correlation was perceived as these have difference Agm/Gal contents, which can influence their biological activity. (Supplementary Figure S5).

The internalization of polyplexes was evaluated via confocal microscopy as this is an effective technique to analyze

siRNA delivery in cell culture (31). Two polymer conjugates from the 10-P library that achieved relative high protein knockdown at low siRNA concentrations ( $[\text{siRNA}] = 0.33 \mu\text{g/ml}$ ), 10-P2 and 10-P3, were selected as representative examples for this analysis. For 10-P2-FA and 10-P3-FA, confocal images showed both punctuated and diffused fluorescence in the interior of the cell 4 h post-transfection. The punctuated fluorescence corresponds to polyplexes localized in cytoplasmic vesicles, while the diffused fluorescence corresponds to polyplexes in the cytosol. These results suggest that the polyplexes were able to successfully escape the cytoplasmic vesicles after cellular internalization, one of the major intracellular barriers to siRNA delivery.

Although polymers of lower  $M_n$  (3 kDa-P) are inclined to be less cytotoxic to cells and more stable in the presence of anionic species, these polymers are less efficient at mediating siRNA transfection. On the other hand, although able to achieve high transfection efficiencies under some conditions, polymers of higher  $M_n$  (21 kDa-P) exhibited more prominent cytotoxicity. Therefore, polymers in the 5 kDa-P and 10 kDa-P libraries are the more promising candidates for siRNA delivery, particularly the P2 and P3 polymers. Our most favorable condition was 5-P3 at a polymer:siRNA (w:w) = 20:1 which showed a good balance between high transfection efficiency and low cytotoxicity. The results obtained for this polymer were superior to PEIb and RNAiFECT, and comparable to TransIT-siQuest; however, a direct comparison with PEIb is more relevant since it is a polymer-based vector.

## CONCLUSIONS

In this work, we developed polymer libraries to help define the structure-function relationships associated with this class of vector. Polymer conjugates were synthesized by the side chain substitution of Agm and Gal to pAA of various  $M_n$ . The biophysical and cellular characterization of these polymeric vectors revealed interesting correlations pertaining to their efficacy as siRNA delivery systems. In general, for this class of polymer conjugates, the higher the Agm content, the more compact and stable the polyplexes and the higher transfection efficiency, but also the higher the cytotoxicity. For polymer conjugates with high Agm content (i.e. P2), higher protein knockdown was correlated to small-sized polyplexes ( $\leq 100 \text{ nm}$ ) and strong binding affinity with siRNA. As for the effect of molecular weight, the lower the polymer  $M_n$ , the more compact and stable the polyplexes and the lower the cytotoxicity, but also the lower the transfection efficiency. Therefore, a critical balance between the polymer  $M_n$  and ligand substitutions, while maintaining a small size ( $\leq 100 \text{ nm}$ ) and strong binding affinity with siRNA, should be attained to optimize the transfection efficiency and maintain high cell viability in culture. Based on these criteria, the most favorable  $M_n$  identified

were 5 kDa and 10 kDa. From these libraries, P2 and P3 polymers were the most effective, particularly 5-P3 which corresponds to a 5 kDa pAA with a side chain composition of 55% Agm and 17% Gal. Characterization of these polymeric vectors allowed the identification of optimal chemical and structural properties, and contributed toward the development of safer and more efficient siRNA delivery systems.

## ACKNOWLEDGMENTS AND DISCLOSURES

We thank the Alfred P. Sloan Foundation Graduate Scholarship Programs and National Action Council for Minorities in Engineering (NACME), Inc. for a Sloan Fellowship (J.M.P.), the Cornell's Learning Initiative in Medicine and Bioengineering (CLIMB) for the National Science Foundation (NSF) GK-12 Fellowship (J.M.P), and the Cornell University NMR and NBTC facilities.

## REFERENCES

1. Fire A, Xu S, Montgomery MK, Kostas SA, Driver SE, Mello CC. Potent and specific genetic interference by double-stranded RNA in *Caenorhabditis elegans*. *Nature*. 1998;391:806–11.
2. Dillon CP, Sandy P, Nencioni A, Kissler S, Rubinson DA, Parijs LV. RNAi as an experimental and therapeutic tool to study and regulate physiological and disease processes. *Annu Rev Physiol*. 2005;67:147–73.
3. Dykxhoorn DM, Lieberman J. The silent revolution: RNA interference as basic biology, research tool, and therapeutic. *Ann Rev Med*. 2005;56:401–23.
4. Shan G. RNA interference as a gene knockdown technique. *Int J Biochem Cell Biol*. 2010;42(8):1243–51.
5. Doody A, Putnam D. RNA-interference effectors and their delivery. *Crit Rev Ther Drug Carrier Syst*. 2006;23(2):134–60.
6. Wiethoff CM, Middaugh CR. Barriers to nonviral gene delivery. *J Pharm Sci*. 2003;92:203–17.
7. Wong SY, Pelet JM, Putnam D. Polymer systems for gene delivery—past, present and future. *Prog Polym Sci*. 2007;32:799–837.
8. Pack DW, Hoffman AS, Pun S, Stayton PS. Design and development of polymers for gene delivery. *Nat Rev Drug Discov*. 2005;4:581–93.
9. Putnam D. Polymers for gene delivery across length scales. *Nat Mater*. 2006;5(6):439–51.
10. Demeneix B, Hassani Z, Behr JP. Towards multifunctional synthetic vectors. *Curr Gene Ther*. 2004;4:445–55.
11. Green JJ, Langer R, Anderson DG. A combinatorial polymer library approach yields insight into nonviral gene delivery. *Acc Chem Res*. 2007;41:749–59.
12. Lynn DM, Anderson DG, Putnam D, Langer R. Accelerated discovery of synthetic transfection vectors: Parallel synthesis and screening of a degradable polymer library. *J Am Chem Soc*. 2001;123:8155–6.
13. Anderson DG, Akinc A, Hossain N, Langer R. Structure/property studies of polymeric gene delivery using a library of poly( $\beta$ -amino esters). *Mol Ther*. 2005;11:426–34.
14. Anderson DG, Lynn DM, Langer R. Semi-automated synthesis and screening of a large library of degradable cationic polymers for gene delivery. *Angew Chem Int Ed*. 2003;42:3153–8.
15. Wong SY, Sood N, Putnam D. Combinatorial evaluation of cations, pH-sensitive and hydrophobic moieties for polymeric vector design. *Mol Ther*. 2009;17:480–90.
16. Thomas M, Lu JJ, Zhang C, Chen J, Klivanov AM. Identification of novel superior polycationic vectors for gene delivery by high-throughput synthesis and screening of a combinatorial library. *Pharm Res*. 2007;24:1564–71.
17. Chen DJ, Majors BS, Zelikin A, Putnam D. Structure-function relationships of gene delivery vectors in a limited polycation library. *J Control Release*. 2005;103:273–83.
18. Pelet JM, Putnam D. An in-depth analysis of polymer analogous conjugation using DMTMM. *Bioconjugate Chem*. 2011;22:329–37.
19. Katas H, Alpar HO. Development and characterisation of chitosan nanoparticles for siRNA delivery. *J Control Release*. 2006;115:216–25.
20. Grayson ACR, Doody AM, Putnam D. Biophysical and structural characterization of polyethyleneimide-mediated siRNA delivery *in vitro*. *Pharm Res*. 2006;23:1868–76.
21. Kolonko EM, Kiessling LL. A polymeric domain that promotes cellular internalization. *J Am Chem Soc*. 2008;130:5626–7.
22. Nakase I, Niwa M, Takeuchi T, Sonomura K, Kawabata N, Koike Y, *et al*. Cellular uptake of arginine-rich peptides: roles for macropinocytosis and actin rearrangement. *Mol Ther*. 2004;10(6):1011–22.
23. Futaki S, Suzuki T, Ohashi W, Yagami T, Tanaka S, Ueda K, *et al*. Arginine-rich peptides. An abundant source of membrane-permeable peptides having potentials as carriers for intracellular protein delivery. *J Biol Chem*. 2001;276:5836–40.
24. Oishi M, Nagasaki Y, Itaka K, Nishiyama N, Kataoka K. Lactosylated poly(ethylene glycol)-siRNA conjugate through acid-labile beta-thiopropionate linkage to construct pH-sensitive polyion complex micelles achieving enhanced gene silencing in hepatoma cells. *J Am Chem Soc*. 2005;127:1624–5.
25. Kunath K, Harpe A, Fischer D, Kissel T. Galactose-PEI-DNA complexes for targeted gene delivery: degree of substitution affects complex size and transfection efficiencies. *J Control Release*. 2003;88:159–72.
26. Zhang X-Q, Wang X-L, Zhang P-C, Liu Z-L, Zhuo R-X, Mao H-Q, *et al*. Galactosylated ternary DNA/polyphosphoramidate nanoparticles mediate high gene transfection efficiency in hepatocytes. *J Control Release*. 2005;102:749–63.
27. Sagara K, Kim SW. A new synthesis of galactose-poly(ethylene glycol)-polyethylenimine for gene delivery to hepatocytes. *J Control Release*. 2002;79:271–81.
28. Hashida M, Takemura S, Nishikawa M, Takakura Y. Targeted delivery of plasmid DNA complexed with galactosylated poly(L-lysine). *J Control Release*. 1998;53:301–10.
29. Nishikawa M, Takemura S, Takakura Y, Hashida M. Targeted delivery of plasmid DNA to hepatocytes *in vivo*: optimization of the pharmacokinetics of plasmid DNA/galactosylated poly(L-lysine) complexes by controlling their physicochemical properties. *J Pharmacol Exp Ther*. 1998;287:408–15.
30. Harada A, Kataoka K. Chain length recognition: core-shell supramolecular assembly from oppositely charged block copolymers. *Science*. 1999;283(5398):65–7. 1999 January 1.
31. Portis AM, Carballo G, Baker GL, Chan C, Walton SP. Confocal microscopy for the analysis of siRNA delivery by polymeric nanoparticles. *Microsc Res Tech*. 2010;73(9):878–85.